Magnetic Resonance Imaging (Including MR Cholangiopancreatography)

Susanne Bonekamp, Celia Pamela Corona-Villalobos, Vivek Gowdra Halappa, and Ihab R. Kamel

Contents

S. Bonekamp · C. P. Corona-Villalobos · V. G. Halappa
I. R. Kamel (✉)
The Russell H. Morgan Department of Radiology and Radiological Sciences, The Johns Hopkins School of Medicine, Baltimore, USA
e-mail: ikamel@jhmi.edu

S. Bonekamp
e-mail: susanne.bonekamp@gmail.com

C. P. Corona-Villalobos
e-mail: ccorona1@jhmi.edu

V. G. Halappa
e-mail: vivekhalappa86@gmail.com

Abstract

Imaging features of biliary tree and primary liver tumors are extremely diverse. Magnetic resonance imaging (MRI) of the liver and MR cholangiopancreatography (MRCP) provide a solid understanding of imaging manifestations useful for accurate detection, characterization, and tumor assessment. Knowledge of tumor characteristics and mimickers is essential for tumor diagnosis and appropriate management. In this chapter, we will discuss the imaging features of biliary tree, gallbladder, and primary liver tumors.

1 Introduction

Magnetic resonance imaging (MRI) is a comprehensive imaging modality with multiplanar capability to assess the liver parenchyma, gallbladder, and biliary tree. MRI provides a comprehensive assessment of the tissue characteristics and vascularity of different pathologies with excellent soft tissue contrast resolution. The addition of magnetic resonance cholangiopancreatography (MRCP) to the MR protocol can help delineate the fluid-filled lumen of the biliary tree and the gallbladder. The diagnostic accuracy of MRCP is comparable to endoscopic retrograde cholangiopancreatography (ERCP) in the diagnosis of biliary pathologies [1–7].

2 Magnetic Resonance Imaging Techniques

Liver MRI protocol typically includes a T1-weighted turbo field-echo in-phase and opposed sequence or a multi-echo Dixon sequence to separate water and fat as well as tissue iron, a breath-hold or respiratory-triggered multishot T2-weighted sequence, diffusion-weighted imaging either respiratory-triggered or breath-held with at least two *b* values, and unenhanced and contrast-enhanced gradient-echo

J. M. Herman et al. (eds.), *Biliary Tract and Gallbladder Cancer*, Medical Radiology. Radiation Oncology,
DOI: 10.1007/978-3-642-40558-7_10,

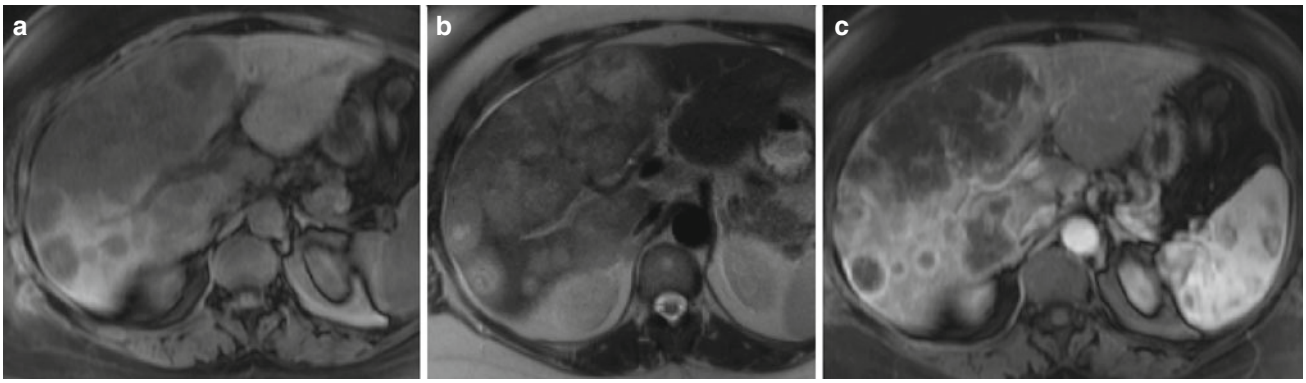

Fig. 1 **a–b** T1- and T2-weighted images show multiple hepatic masses throughout the liver, with a more confluent area of tumor within the inferior right hepatic lobe consistent with metastatic cholangiocarcinoma. These lesions demonstrate rim enhancement on **c** arterial phase

(GRE) T1-weighted imaging sequences, which can be either acquired at predetermined time points, i.e., arterial phase (20–25 s), portal venous phase (60 s), delayed phase (3 min), or using a bolus-tracking technique to determine the patient-specific timing of the different post-contrast phases. This protocol provides comprehensive overview, which allows the detection of hepatic or biliary malignancies, with diffusion and contrast-enhanced sequences providing a noninvasive assessment of the vascularity, viability, and cell density of the tissue and suspected malignancy.

MRCP is performed using breath-hold (using a single-shot approach) or non-breath-hold techniques (with respiratory triggering) two-dimensional (2D) or three-dimensional (3D) T2-weighted sequences. A 3D technique provides a higher signal-to-noise ratio (SNR), which is traded off for thinner contiguous slices. Acquiring images with near isotropic voxels allows improved post-processing manipulation of the images with multiplanar reconstruction, maximum intensity projection (MIP), and volume rendering. The introduction of faster gradients and a parallel acquisition technique has resulted in even greater spatial resolution and faster acquisition times. Often, patients fast for at least 4 h in order to reduce fluid secretions within the stomach and duodenum, reduce bowel peristalsis, and promote gallbladder distension. Sometimes, a negative oral contrast agent (e.g., iron oxide or blueberry juice) is used to reduce the signal intensity of overlapping fluid within the stomach and duodenum. Recently, functional assessment of biliary excretion has become possible with the use of hepatobiliary contrast media by T1-weighted sequences for MRCP.

Hepatobiliary contrast agents include, historically, mangafodipir trisodium (Teslascan; Nycomed Amersham), gadobenate dimeglumine (Gd-BOPTA, MultiHance; Bracco Imaging), and gadolinium ethoxybenzyldiethylenetriamine penta-acetic acid (Gd-EOB-DTPA, Eovist; Bayer Healthcare). These contrast agents can provide standard arterial, portal venous, and equilibrium phase images with an added hepatobiliary phase 10–20 min after contrast injection for Gd-EOB-DTPA and 1 h after contrast injection for Gd-BOPTA. Furthermore, delayed imaging in the axial and coronal planes, 10–120 min after contrast administration, results in hyperintense bile on T1-weighted fat-saturated images. The advantages of functional MRCP compared to classical T2-weighted MRCP are effective in evaluation of biliary anatomy [8], improved visibility communications between cystic lesions and draining bile ducts in the diagnosis of congenital biliary disorders [9, 10], differentiation of biliary from extrabiliary lesions [8], improved diagnostic accuracy of true obstruction in a dilated biliary system compared pseudo-obstruction [11], and better detection of post-operative complications including depiction of active extravasation of contrast in suspected bile leaks [10, 12].

3 Cholangiocarcinoma

Cholangiocarcinomas are a distinct type of tumors that originate from the biliary epithelium either within the liver or within the biliary tract (Fig. 1). Grossly, cholangiocarcinoma is a firm hypovascular tumor with predominantly fibrous stroma, and, histologically, it is a well-differentiated adenocarcinoma with desmoplasia. There are various recognized risk factors for cholangiocarcinoma; infections with liver flukes and hepatolithiasis are considered common in endemic areas. Endogenous and dietary nitrosamine compounds associated with parasitic infections act as cofactors in carcinogenesis owing to the carcinogenic effect of nitrosamine compounds on the proliferation of epithelial cells of the bile duct [13, 14]. In the western world, most common risk factors for cholangiocarcinoma include primary sclerosing cholangitis, hepatic cirrhosis, chronic hepatitis C infection, alcoholic liver disease, chronic inflammatory bowel disease, and diabetes [15, 16]. MR imaging and MRCP are very useful in the diagnosis and

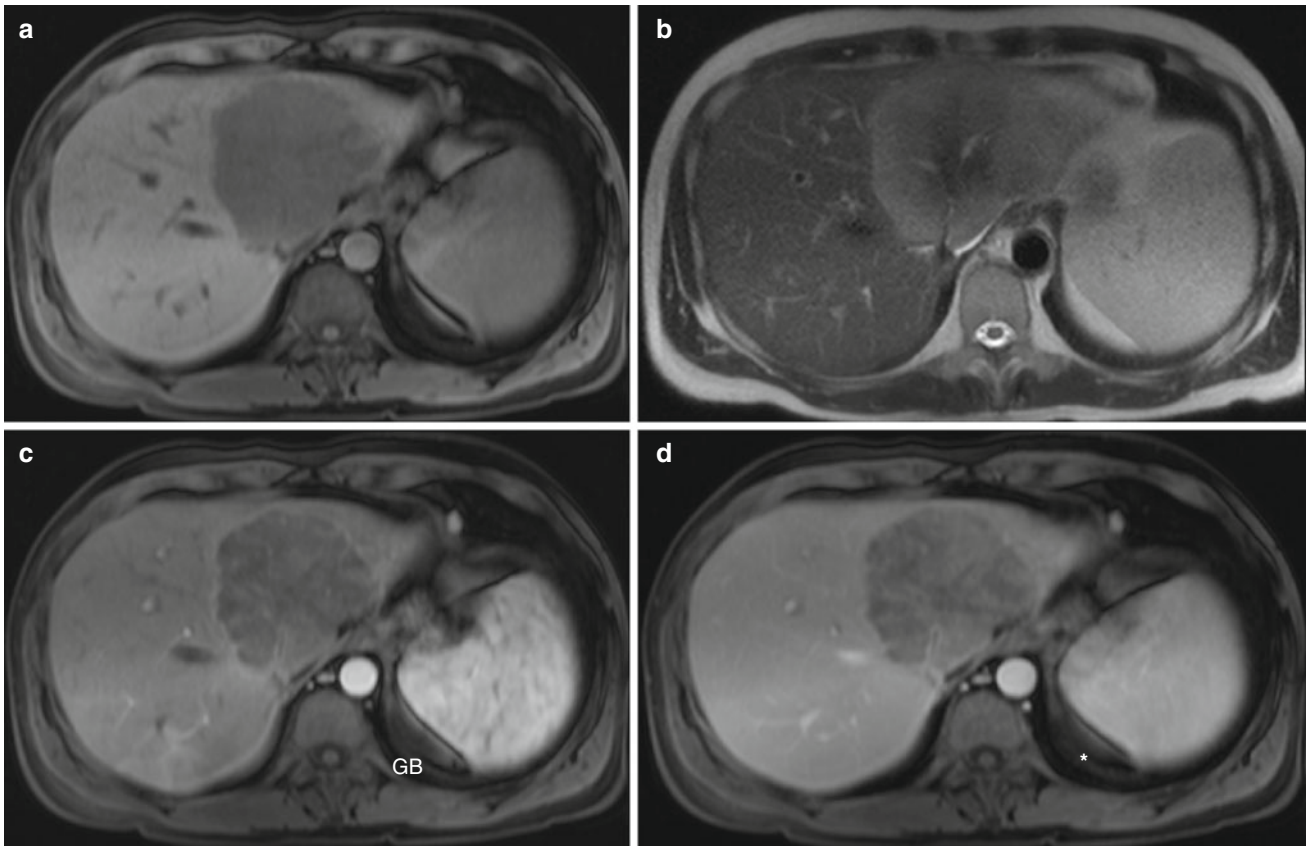

Fig. 2 A 73-year-old male diagnosed with cholangiocarcinoma. There is a heterogeneous mass of approximately 8 × 5.5 cm to the left of the falciform ligament involving the left and anterior right hepatic lobes. The left and middle hepatic veins are occluded. The mass demonstrates irregular borders predominantly hypointense in **a** T1- and **b** T2-weighted images. There is rim irregular enhancement of the mass after contrast administration in **c** arterial and **d** venous phases with presence

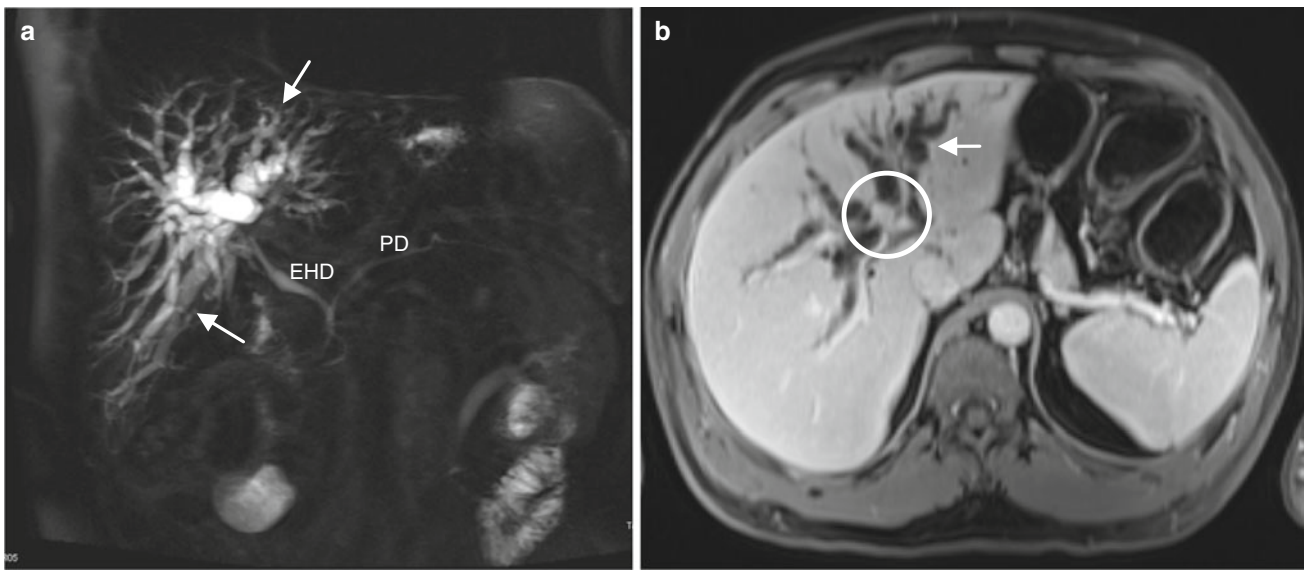

Fig. 3 **a** MRCP shows marked intrahepatic biliary dilatation or the right and left ducts (*arrows*); the pancreatic duct (*PD*) and the extrahepatic biliary duct (*EHD*) are normal. **b** Delayed contrast-enhanced image depicts an abrupt transition point at the porta hepatis showing a nodular area of enhancement (*circle*) due to a small tumor demonstrated by brushing

assessment of resectability in cholangiocarcinoma and to visualize surrounding bile ducts, vessels, and hepatic parenchyma owing to its intrinsic high tissue contrast and multiplanar capability [17, 18]. MR imaging consists of axial and coronal T2-weighted images, fat-sat T1-weighted images, dynamic contrast-enhanced T1-weighted images (DCE-MR), and MRCP. T2-weighted images and T1-weighted MR images are useful in detection and characterization of the tumor (Fig. 1), DCE-MR is useful in differentiating benign from malignant strictures, and MRCP is useful in evaluating periductal-infiltrating or intraductal-growing-type cholangiocarcinoma (Figs. 2 and 3) .

Cholangiocarcinoma is broadly classified into (1) extrahepatic and (2) intrahepatic cholangiocarcinoma (ICC).

3.1 Intrahepatic Cholangiocarcinoma

ICC is the second most common primary malignancy of the liver behind hepatocellular carcinoma (HCC). Based on the morphology and growth patterns, cholangiocarcinoma has been classified into three types: (1) mass-forming (2) intraductal-growing, and (3) periductal-infiltrating types [19].

Dynamic contrast-enhanced MR imaging findings in cholangiocarcinoma, in general, include early rim enhancement, characteristic delayed and persistent enhancement of the tumor. These findings reflect the characteristic fibrous content in the tumor and delayed diffusion of the contrast through the tumor interstitium [20]. On Gd-EOB-DTPA-enhanced MRI (Eovist), ICC presents as a hypointense lesion in delayed phase. Images in the hepatobiliary phase demonstrate highest lesion conspicuity with high contrast-to-noise ratio (CNR), and there will be no liver-specific contrast uptake since there will be negligible increase in SNR from late venous to hepatobiliary phases [21].

3.2 Intrahepatic Cholangiocarcinoma: Mass-Forming Type

Mass-forming cholangiocarcinoma presents as a homogenous mass with irregular, well-defined margins often associated with dilatation of the biliary trees in the periphery (Fig. 4). On MR imaging, the mass demonstrates irregular margins with high signal intensity on T2-weighted imaging and low signal intensity on T1-weighted imaging. On T2-weighted images, there may be a central hypointense area, which probably reflects severe fibrosis. On post-contrast MR images, there will be irregular peripheral enhancement with concentric filling of contrast material [22]. Significant central enhancement can be seen in delayed phase MR imaging, and this may be, again, due to the fibrous stroma of the tumor. Atypical presentations such as homogenous hypervascular enhancement, strong hyperintensity, and centripetal enhancement on T2-weighted MR images can be seen in mucinous carcinoma, but it presents with continuous ragged rim enhancement, which can help differentiate it from a hemangioma.

3.3 Intrahepatic Cholangiocarcinoma: Periductal-Infiltrating Type

Periductal-infiltrating type of cholangiocarcinoma usually presents as a growth along a dilated or narrowed bile duct without mass formation and as an elongated or branchlike abnormality. Early diagnosis of periductal-infiltrating type of cholangiocarcinoma may be difficult since it may appear to be a benign looking stricture in the early stages. It is important to differentiate a benign from a malignant stricture and findings such as stricture with an irregular margin, asymmetric narrowing, lymph node enlargement, enhancing ducts, and periductal soft tissue lesion should raise strong suspicion for a malignant stricture [6]. On MR imaging, periductal-infiltrating type of cholangiocarcinoma presents with diffuse periductal thickening and increased enhancement due to tumor infiltration with abnormally dilated or irregularly narrowed duct and peripheral ductal dilatation [23] (Figs. 5 and 6).

3.4 Intrahepatic Cholangiocarcinoma: Intraductal-Growing Type

Intraductal-growing-type cholangiocarcinoma has a significantly better prognosis than mass-forming-type or periductal-infiltrating-type cholangiocarcinoma (Fig. 7). MR imaging features suggestive of intraductal-growing-type cholangiocarcinoma include (1) papillary or irregular polypoid shape, (2) lack of constriction of the tumor-bearing segment, (3) hypoenhancement of the tumor to the liver during the equilibrium phase, (4) tumor multiplicity, (5) upstream and downstream bile duct dilatation, and (6) no bile duct wall thickening adjacent to the tumor. Kim et al. suggested that the presence of at least two of these six imaging features, when used in combination, has a sensitivity and specificity in the diagnosis intraductal-growing-type cholangiocarcinoma of 95 and 70 %, respectively. Intraductal-growing-type cholangiocarcinoma has a tendency to spread superficially along the mucosal surface, resulting in multiplication. Intraductal-growing-type cholangiocarcinoma more often showed washout, whereas mass-forming cholangiocarcinoma more often showed gradual persistent or progressive enhancement, which will help in differentiating between the two [24] (Figs. 8 and 9).

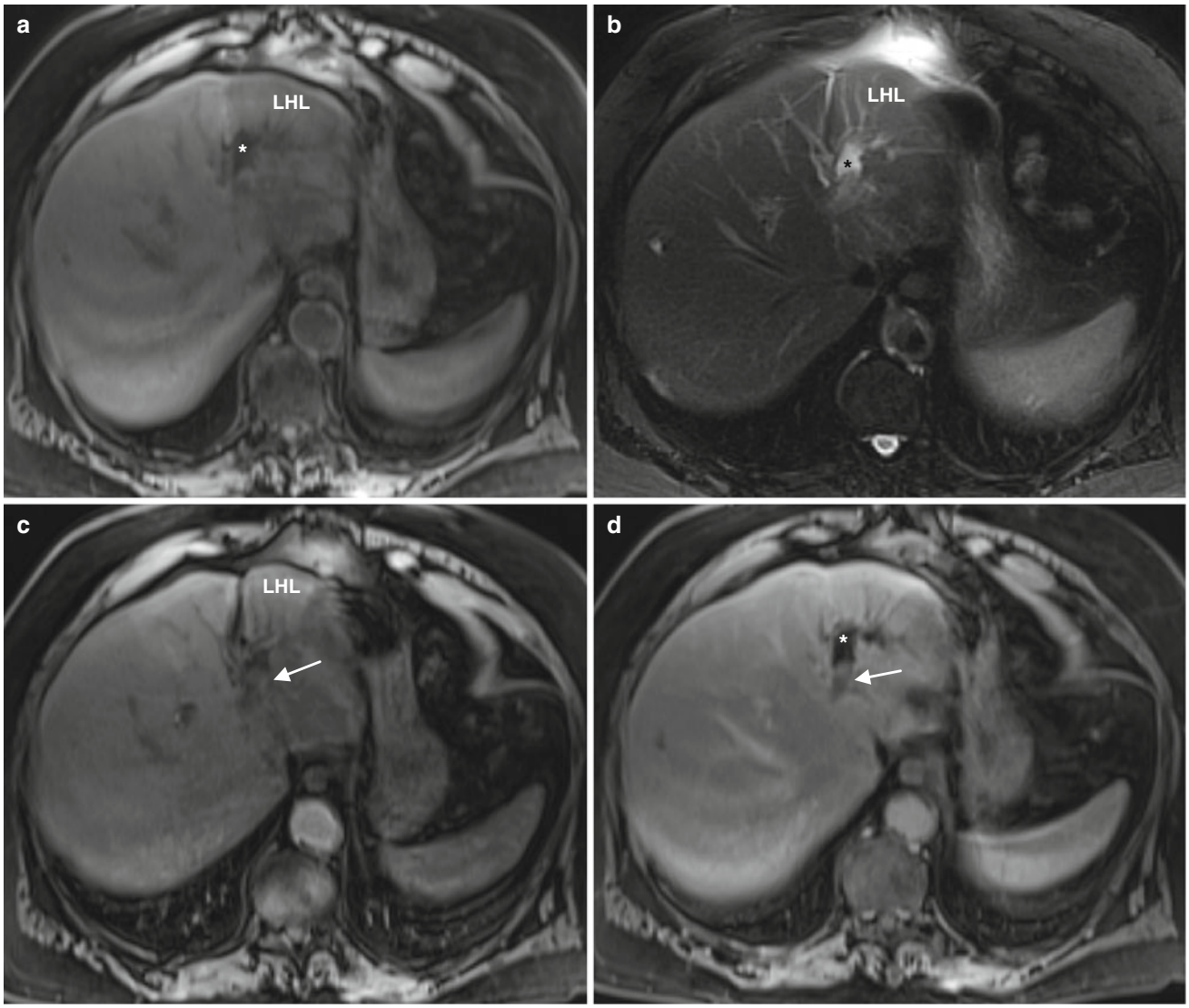

Fig. 4 **a** T1-weighted and **b** T2-weighted images demonstrate atrophy of the left hepatic lobe (*LHL*) with intrahepatic biliary dilatation (*). The biliary dilatation terminates at the level of an enhancing mass (*arrows*) in the left lobe as shown in the arterial **c** and venous phases **d** consistent with cholangiocarcinoma

3.5 Extrahepatic Cholangiocarcinoma

Extrahepatic cholangiocarcinoma arises from the ductal epithelium of the extrahepatic bile duct. The most important factors in evaluating patients with extrahepatic cholangiocarcinoma are to determine tumor location and its longitudinal extent since these factors have greatest influence on surgical method and survival [13]. MRI is one of the most important diagnostic imaging modalities of choice used in assessing the longitudinal and lateral spread of a tumor when determining resectability. Perihilar cholangiocarcinomas have been categorized into four types by the modified Bismuth–Corlette classification adapted from the original classification [25]. On MR imaging, the enhancement pattern of extrahepatic cholangiocarcinomas is similar to that of ICCs. The tumors are hypovascular and enhance slowly and gradually to a peak on delayed imaging. These tumors are less heterogeneous than ICC since they present as small infiltrating tumors. Satellite nodules and central scars are unusual compared to ICC. Extrahepatic cholangiocarcinoma typically presents as abnormal circumferential extrahepatic bile duct wall thickening and enhancement best visualized 1–5 min after gadolinium administration [26].

On diffusion-weighted imaging, extrahepatic cholangiocarcinoma demonstrates differential levels of high signal intensity and low signal intensity in apparent diffusion coefficient maps and has great sensitivity in detection of extrahepatic cholangiocarcinoma comparable to MRCP [27].

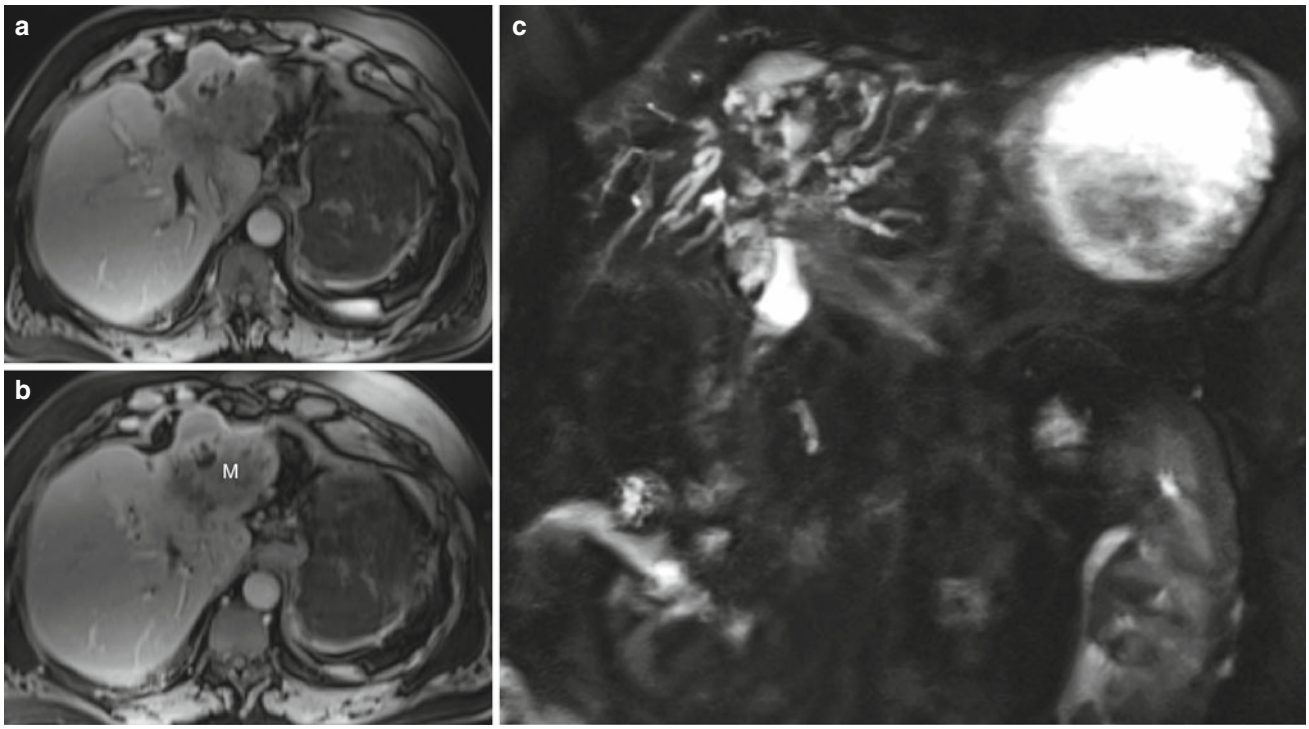

Fig. 5 There is a hypointense ill-defined 9.4 × 6.2 cm mass within the left hepatic lobe associated with atrophy of the left hepatic lobe. After contrast administration, there is heterogeneously rim enhancement in **a** portal and **b** delayed phases. **c** MRCP shows intrahepatic biliary ductal dilatation in the right and left hepatic lobes

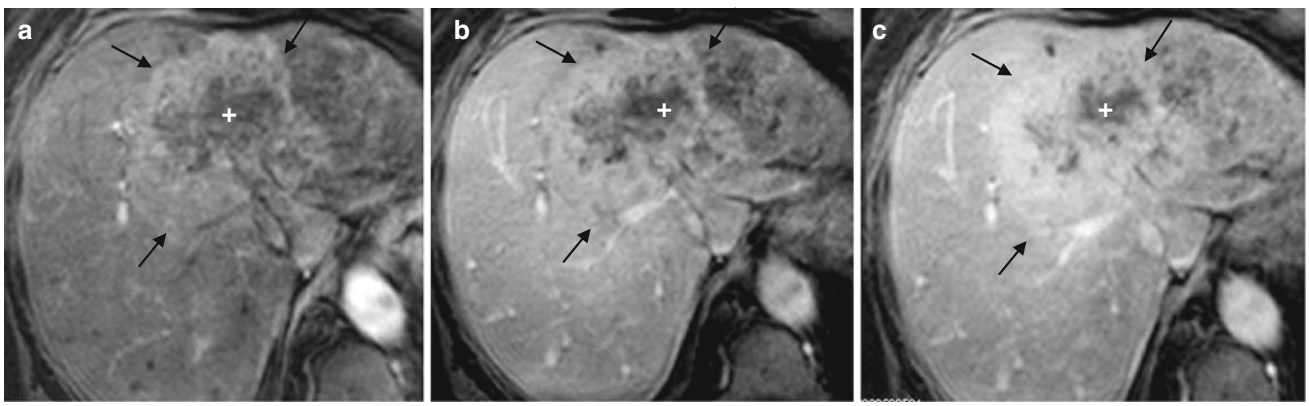

Fig. 6 A 66-year-old female diagnosed with intrahepatic cholangiocarcinoma. There is a large heterogeneously infiltrating mass involving the right and left hepatic lobes. **a–c** after contrast administration enhanced images showed peripheral enhancement (*arrows*) and central hypointense region probably associated with necrosis (+)

3.6 Hilar Cholangiocarcinoma/Klatskin Tumors

Hilar cholangiocarcinoma, also known as Klatskin tumors, are adenocarcinomas that arise at the confluence of the right and the left hepatic bile ducts. MRI and MRCP can provide accurate preoperative staging of biliary tree, liver, and vascular involvement, and this is crucial in choosing the most appropriate treatment option in patients with cholangiocarcinoma.

Hilar cholangiocarcinoma demonstrates circumferential growth and spreads along the bile ducts with poor conspicuity on non-contrast MR images [28]. Hilar cholangiocarcinoma presents with the same signal intensity as peripheral tumors on both T1- and T2-weighted images. On post-contrast images, hilar cholangiocarcinomas do not

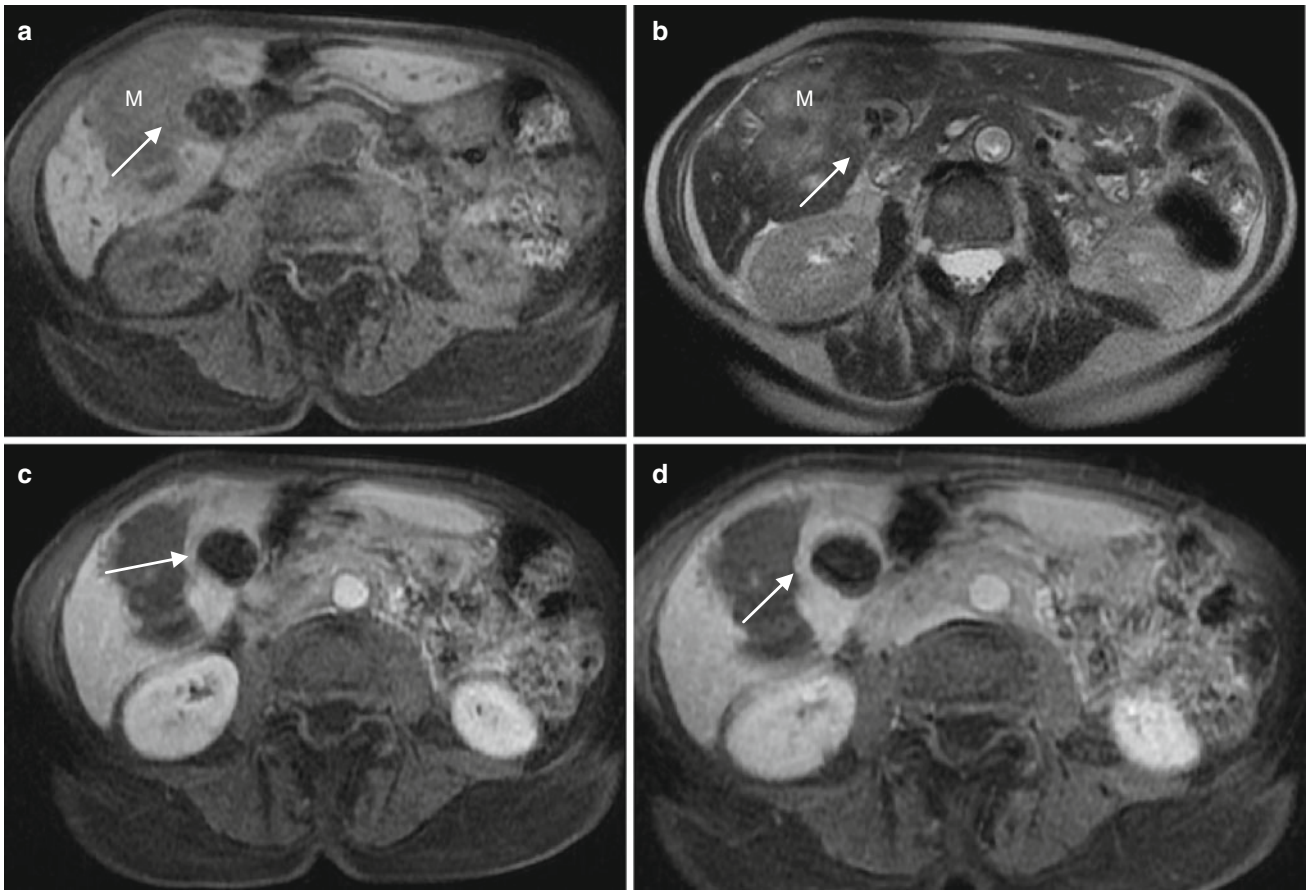

Fig. 7 A 73-year-old female with history of metastatic cholangiocarcinoma. **a** T1 image shows a dark infiltrative mass with irregular border on the right hepatic lobe. On **b** T2-weighted image, the mass looks heterogeneously hyperintense. After contrast administration, **c** portal and **d** delayed images showed peripheral enhancement. The mass appears contiguous with the gallbladder fundus with associated thickening of the fundus (*arrows*) and gallbladder stones

always show a unique enhancement pattern. Most of the lesions are hypovascular compared to the adjacent liver parenchyma, with a heterogeneous enhancement that gradually peaks on delayed phase images, which is due to the fibrous nature of the tumor [29]. Some lesions show periductal enhancement, whereas very few hilar cholangiocarcinoma are hypervascular, but they do not demonstrate immediate diffuse enhancement unlike other hypervascular lesions.

3.7 Mixed Hepatocellular carcinoma–Cholangiocarcinoma

Mixed hepatocellular carcinoma–cholangiocarcinoma (HCC-CC) contributes to a small but significant proportion of primary liver malignancies, and they are comprised of cells with histopathological features of both cholangiocarcinoma and HCC [30].

On MRI, mixed hepatocellular carcinoma–cholangiocarcinoma usually presents with a single mass, moderately high signal intensity on T2, tumor demonstrating progressive enhancement or contrast retention, and frequent lack of capsule. Enhancement patterns include early rim enhancement and diffuse heterogeneous enhancement [31]. Hwang et al. demonstrated that on Gadoxetic acid-enhanced MRI, irregular shape, strong rim enhancement during early dynamic phase MRI, and absence of target appearance on hepatobiliary phase were more suggestive of hepatocellular carcinoma–cholangiocarcinoma (HCC-CC), whereas the findings of a lobulated shape, weak peripheral rim enhancement, and presence of complete target appearance on the hepatobiliary phase were more of suggestive ICC [32].

- Differential Diagnosis:
  Variety of neoplastic and non-neoplastic conditions can mimic the findings of cholangiocarcinoma and, thus, poses significant challenges in the diagnosis and management of these patients.
- Neoplastic Conditions:
  A tumors that should be considered in the differential diagnosis of cholangiocarcinoma includes HCCs. Patients

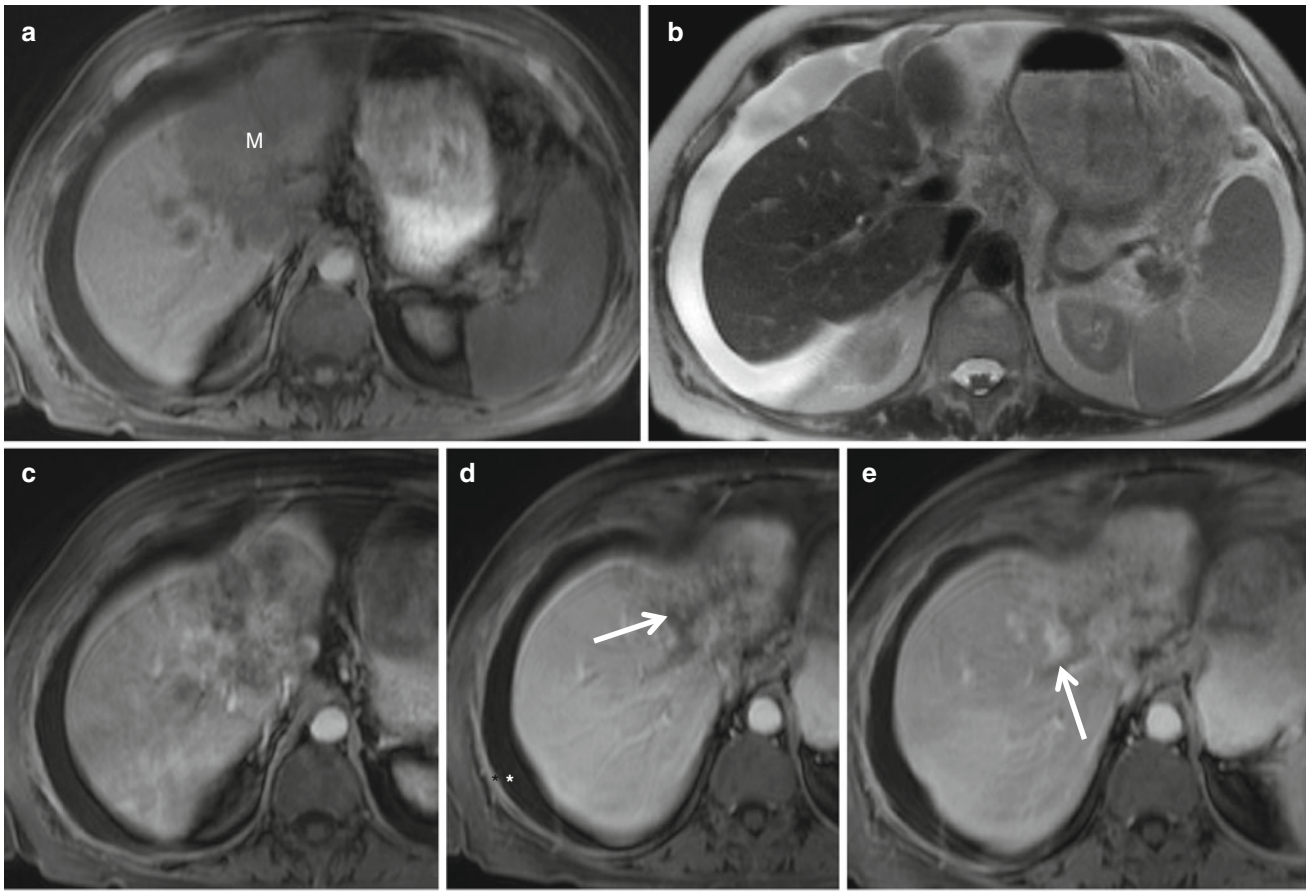

Fig. 8 Shrinkage of left hepatic lobe is noticed. **a** T1-weighted image shows a hypointense mass (*M*), which nearly replaces the entire left lobe of the liver, and it measures 8 × 7 cm. There is mild intrahepatic biliary duct dilatation (arrows). After contrast administration (**c**–**e**), there is late and heterogeneously enhancement of the mass. There is ascites seen in abdomen (*)

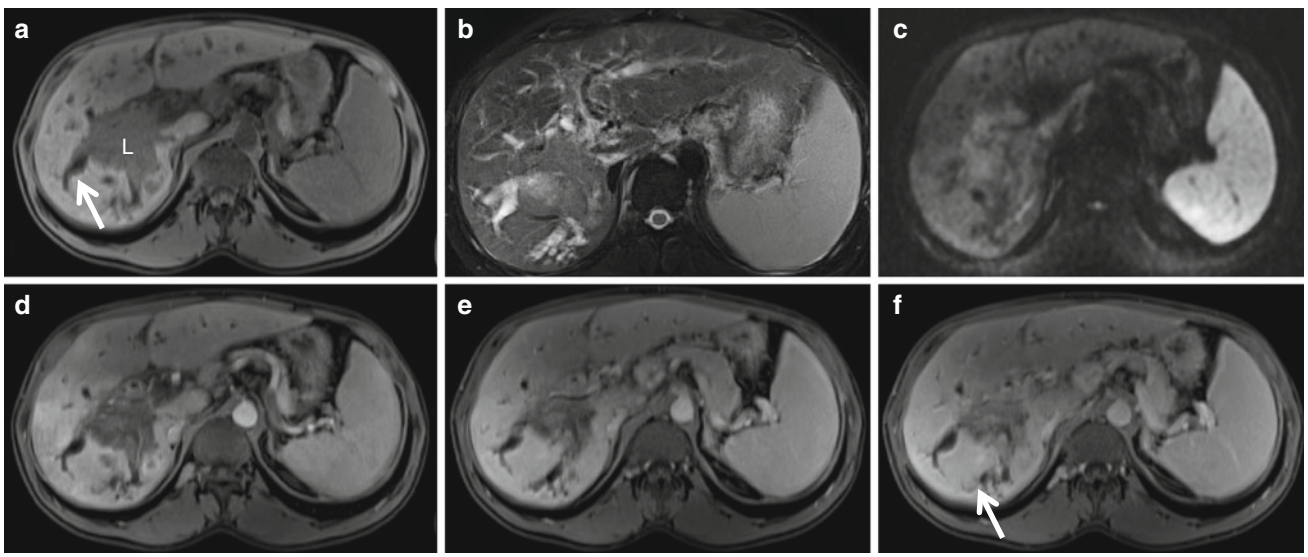

Fig. 9 A 33-year-old male with diagnosis of cholangiocarcinoma. There is a (**a**) T1 hypointense (**b**) T2, and (**c**) diffusion hyperintense infiltrative lesion (*L*) with (**d**–**f**) delayed enhancement near to the porta hepatis extending to the right hepatic lobe. There is severe intrahepatic biliary ductal dilatation proximal to the lesion involving the entire right hepatic lobe (*arrows*)

where clinical background of cirrhosis, hepatitis B/C positive serology, and/or high levels of alpha feto protein (AFP) should alert toward the suspicion of HCC. According to the American Association for the Study of Liver Diseases (AASLD), diagnosis of HCC is to be considered in a mass larger than 2 cm with typical features of hypervascularity in the arterial phase and washout in the venous phase on a contrast-enhanced computed tomography or magnetic resonance (MR) imaging. A mass measures 1–2 cm is also considered suspicious for HCC if it shows these features at both CT and MRI. Park et al. demonstrated that a target appearance, with central enhancement and a hypointense rim on diffusion-weighted imaging (DWI), proved to be a reliable imaging marker indistinguishing small mass-forming an ICC from a small HCC [33].

Other neoplastic conditions to be considered in the differential diagnosis include intrabiliary metastases. Although rare, if suspected, metastasis from colonic adenocarcinoma tops the list since it shows increased predilection for biliary ducts [34]. Biliary tract melanoma can either be a primary melanoma arising from the biliary epithelium or metastasis from elsewhere. Owing to its own melanin content, this mass may demonstrate high signal intensity on T1-weighted images and low signal intensity on T2-weighted images [35]. Lymphoma of the bile ducts is very rare and usually a secondary manifestation of systemic disease. Most biliary lymphomas are non-Hodgkin's lymphomas. Carcinoid tumors of the bile ducts are rare and account for less than 2 % of gastrointestinal carcinoid tumors. Imaging findings vary and are non-specific, including biliary strictures with associated wall thickening or a large exophytic mass, thus mimicking the periductal-infiltrating or mass-forming types of cholangiocarcinoma.

- Non-neoplastic Conditions:
  Various conditions that mimic cholangiocarcinoma on imaging include primary and secondary sclerosing cholangitis (SSC) and Mirizzi syndrome. MR cholangiopancreatography (MRCP) is considered the best initial approach in the diagnosis of primary sclerosing cholangitis (PSC) and characteristic imaging findings suggestive of PSC include multifocal strictures, irregular beading of the intra- and extrahepatic bile ducts, segmental ectasia, and ductal wall thickening [36]. SSC represents various disorders that are similar to PSC resulting from distinct pathologic process and include recurrent pyogenic cholangitis, which presents in the setting of biliary obstruction by stones or biliary strictures with recurrent episodes of acute pyogenic cholangitis and usually affects the extrahepatic duct, lateral segment of the left lobe, and posterior segment of the right lobe. MR imaging findings characteristic of recurrent pyogenic cholangitis include biliary strictures, intraductal pigmented stones, and ductal wall thickening due to fibrosis [37]. Mirizzi syndrome occurs due to the obstruction of the common hepatic duct due to compression by a gallstone impacted at the gallbladder neck or cystic duct, and it is considered that a low insertion of the cystic duct into the common hepatic duct is a predisposing factor for Mirizzi syndrome [38]. MRCP is a useful imaging modality in detecting gall stones and bile duct stenosis. Although imaging findings may not be specific, MRCP imaging findings suggestive of Mirizzi syndrome include presence of gallstone in the cystic duct, extrinsic narrowing of the common hepatic duct, dilatation of the intrahepatic and common hepatic ducts, and a normal common bile duct. In some cases, there will be strictures secondary to inflammation around the common bile duct and, thus, can resemble cholangiocarcinoma of the periductal-infiltrating type [39].

Another condition that resembles periductal-infiltrating-type cholangiocarcinoma is autoimmune pancreatitis–cholangitis. It presents with focal or diffuse strictures of the pancreatic ducts and the bile ducts. Narrowing of the intrapancreatic bile duct and bile duct strictures with upstream ductal dilatation can be seen resembling the periductal-infiltrating-type cholangiocarcinoma on MRI. The presence of pancreatic abnormalities, which include focal/diffuse/sausage-shaped diffuse enlargement of the pancreas with a peripheral hypoattenuating halo, should favor the diagnosis of autoimmune pancreatitis [40].

MRCP has been demonstrated to be a useful noninvasive imaging modality comparable to ERCP in differentiating extrahepatic bile duct cholangiocarcinoma from benign stricture. Based on cholangiographic criteria described by Park et al. [6] for malignant biliary strictures, irregular margins, and asymmetric narrowing were more commonly found in cholangiocarcinomas than in biliary strictures.

4 Periampullary Tumors

Periampullary tumors are neoplasms that arise within 2 cm of the major duodenal papilla and include pancreatic head carcinoma, intrapancreatic bile duct carcinoma, and periampullary duodenal carcinoma. While they share an anatomic location and clinical presentation, each malignancy has a different prevalence and outcome. While obstructive jaundice is the most common clinical symptom, the major changes seen on cross-sectional imaging are pancreaticobiliary duct dilatation, double duct sign, three-segment sign, four-segment sign, and shape and wall thickness of the distal margins of the common bile duct and the main pancreatic duct [41–43]. Periampullary tumors appear as low signal intensity masses in the region of the ampulla on T1-weighted fat-suppressed MRI. Most

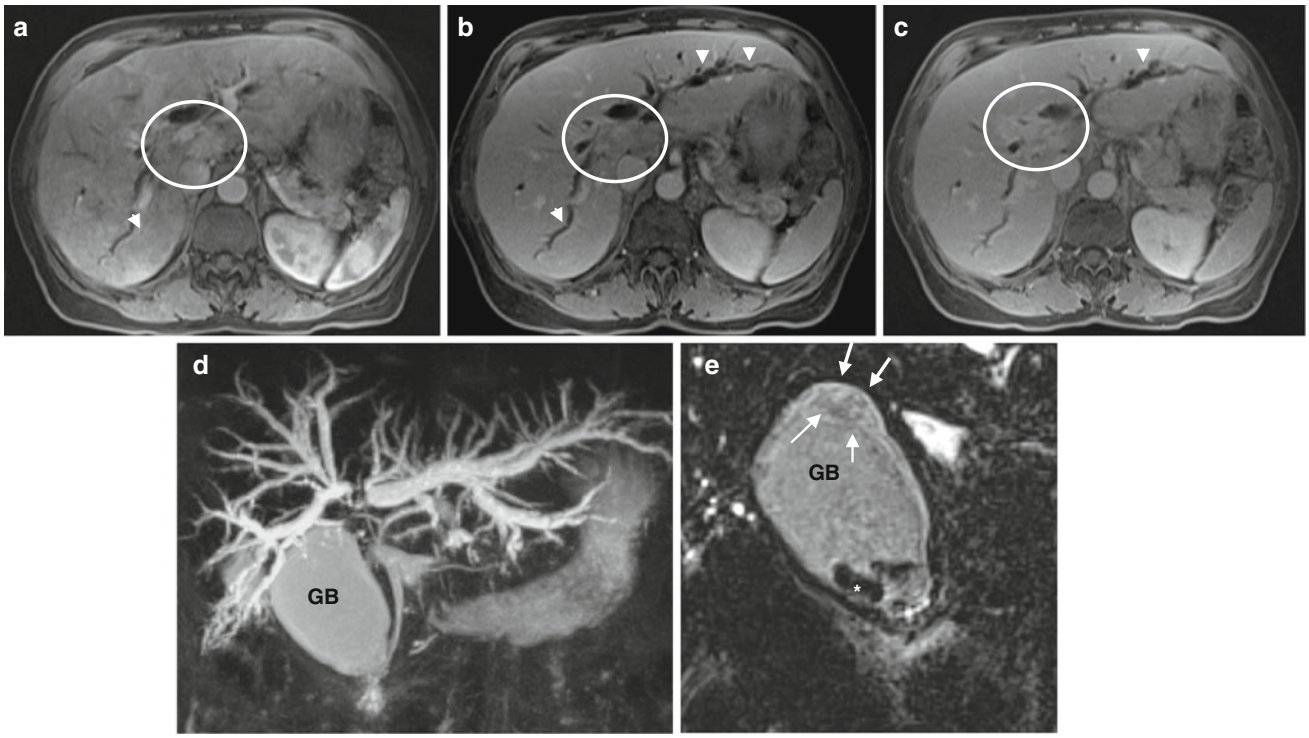

Fig. 10 A 69-year-old male with diagnosis of metastatic gallbladder adenocarcinoma. Contrast-enhanced MRI demonstrates (**a**–**c**) extensive intrahepatic ductal dilatation (*arrowheads*) with abrupt truncation at the hilar region related to an infiltrating mass measuring 4.2 × 2.6 cm (*circle*). On the delayed image (**c**), there is enhancement of the mass at the hilar level. MRCP (**d**) shows a distended gallbladder (GB) with intrahepatic ductal dilatation of the biliary tree. **e** There is diffuse wall thickening more pronounce at the fundus (*arrows*) and presence of choleithiasis (*)

lesions are hypovascular with low signal intensity relative to adjacent normal tissue on contrast-enhanced T1-weighted images; however, a thin rim of peripheral enhancement can often be found on these fat-suppressed images. MRCP helps determine the precise location and organ of origin of these tumors. MR imaging can not only be used to differentiate these lesions, but also to assess resectability [44].

5 Ampullary Carcinoma

Ampullary carcinoma is often considered part of the group of periampullary tumors. They are small tumors arising in the ampulla of Vater that often cause biliary outflow obstruction. Diagnosis can be difficult because these small tumors mimic the appearance of benign causes of biliary outflow obstruction such as papillitis, papillary stenosis, and sphincter of Oddi dysfunction [41, 45–47]. Classical signs of ampullary carcinoma seen on MRI with MRCP are the presence of an ampullary mass, papillary bulging, irregular and asymmetric common bile duct narrowing, and proportional biliary dilatation [41, 46, 47]. MRCP can detect ampullary carcinoma with a high sensitivity (100 %), but limited specificity (59.1–63.6 %) [45]. The addition of diffusion-weighted MRI has been shown to improve detection in a recent study [48].

6 Gallbladder Carcinoma

Primary carcinoma of the gallbladder is the fifth most common tumor of the gastrointestinal tract [49]. Gallbladder carcinoma is a highly malignant tumor with a poor 5-year survival rate of less than 5 % [50]. Gallbladder carcinoma is more common in women than in men; this predilection is thought to be associated with a higher incidence of cholelithiasis. Up to 80 % of gallbladder carcinomas are associated with gallstones, and the risk seems to be associated with stone size [51]. Stones with diameter greater than 3 cm are detected more frequently in gallbladder carcinoma, suggesting a pathogenic role in the gallbladder epithelium carcinogenesis (Fig. 10) [50]. Chronic inflammation of the gallbladder by biliary components such as bile acids, bilirubin, and cholesterol also plays a pathogenic role in gallbladder malignant transformation [52].

Other risk factors are polypoid lesions (>10 mm), an anomalous junction of pancreaticobiliary ducts (AJPBD), especially without choledochal cyst, and aa porcelain gallbladder in up to 25 % of cases [51]. Gallbladder polyps are predisposing factors for gallbladder carcinoma with a prevalence of 3–6 %. This prevalence increases with polyp size (>15 mm, 46–70 %), number (solitary, 80–100 %), shape (sessile, 30 %), and echogenicity (isoechoic or echopenic) of the polypoid lesion [50]. AJPBJ is a congenital defect in the union of pancreatic and biliary ducts; this condition is associated with gallbladder cancer in approximately 10 % of patients, particularly in patients without cystic dilatation of the common bile duct [53]. Calcification of the gallbladder wall, known as "porcelain gallbladder," is associated with approximately 20 % of gallbladder carcinomas. Patients with incomplete calcification of the gallbladder will be at higher risk than those with complete mucosal calcifications. However, the relationship of calcification to malignancy has not been well established.

Less important associated conditions are chronic bacterial infections (Escherichia coli, Opisthorchis viverrini), typhoid carrier state (Salmonella typhi or paratyphi), occupational environmental carcinogens, hormonal changes in women, and familial factors. Clinical presentation in patients with gallbladder carcinoma is non-specific including abdominal pain, weight loss, jaundice, and fever [54]. Carcinoembryogenic antigen values higher than 4 ng/mL in the appropriate clinical setting are 93 % specific but 50 % sensitive for diagnosis [55]. Clinical and radiological diagnosis of gallbladder carcinoma is essential in patients with increased risk of developing tumors and in surgical planning. Gallbladder carcinoma is typically classified according to its appearance as (1) intramural polypoid mass, (2) focal or diffuse asymmetrical gallbladder wall thickening, and (3) occupying the gallbladder fossa [56].

6.1 Intramural Polypoid Mass

Intramural polypoid mass is the least common form, representing 15–25 % of gallbladder carcinomas [54]. Usually well-differentiated and confined to the muscular layer, this variety tends to expand into the lumen of the gallbladder before invading the wall. Lesions are usually ≥1 cm in size and can be mistakenly considered adenomatous or hyperplastic cholesterol polyps, adenomas, non-shadowing stones, or metastases from melanoma. T1-weighted images demonstrate polypoid mass with intermediate signal intensity arising from the thickened wall of the gallbladder. On T2-weighted images, the mass demonstrates high signal intensity. Polypoid lesions show moderately early enhancement, which persist through the portal phase, while benign lesions usually wash out [57].

6.2 Focal or Diffuse Asymmetric Gallbladder Wall Thickening

Focal or diffuse asymmetric gallbladder wall thickening represents 20–30 % of the gallbladder carcinomas. Focal or diffuse thickening of more than 10 mm is highly suspicious. This variant is difficult to differentiate from acute or chronic cholecystitis, xanthogranulomatous cholecystitis, adenomyomatosis, hepatitis, portal hypertension, and congestive heart failure [58]. The tumor is usually seen on MRI as a diffuse asymmetric, extensive irregular thickened wall heterogeneously hyperintense relative to the liver on T2-weighted and iso- or hypointense in T1-weighted images. All gallbladder tumors show conspicuous arterial enhancement after contrast administration, which is irregular in the early phase [59] and persists or becomes isointense to the liver during portal venous phase [60]. However, these characteristics may overlap with benign conditions.

6.3 Subhepatic Mass Occupying the Gallbladder Fossa

Subhepatic mass occupying the gallbladder fossa is the most common form, representing 40–65 % of gallbladder carcinomas [56]. This variant tends to occupy nearly the entire lumen of the gallbladder, often invading the surrounding liver parenchyma, which is highly suggestive of gallbladder carcinoma. MRI usually shows hypo- to isointense signal intensity on T1-weighted and heterogeneously hyperintense signal intensity on T2-weighted images [56] (Fig. 11). Tumors show avid irregular enhancement on the periphery of the lesion during arterial phase and tend to maintain the enhancement throughout the portal and delayed phase, which facilitates differentiation from HCCs. Post-contrast fat-suppressed T1-weighted images are useful for tumor extent and vascular invasion.

6.4 Lymphoma of the Gallbladder

Lymphomas of the gallbladder are extremely rare. To date, there are only 50 cases of primary lymphoma of the gallbladder reported in the literature [61]. Of these, most reported cases of gallbladder lymphoma are diffuse large B cell or mucosa-associated lymphoid tissue types. Chronic lymphocytic leukemia, small lymphocytic lymphoma, and follicular lymphoma are exceedingly rare. Cases are reported in elder patients, and the majority of patients present clinical symptoms of cholecystitis or cholelithiasis. Radiological findings in previous reports have shown wall thickening associated with intramural mass formation [62]. Differentiation between lymphoma of the gallbladder and

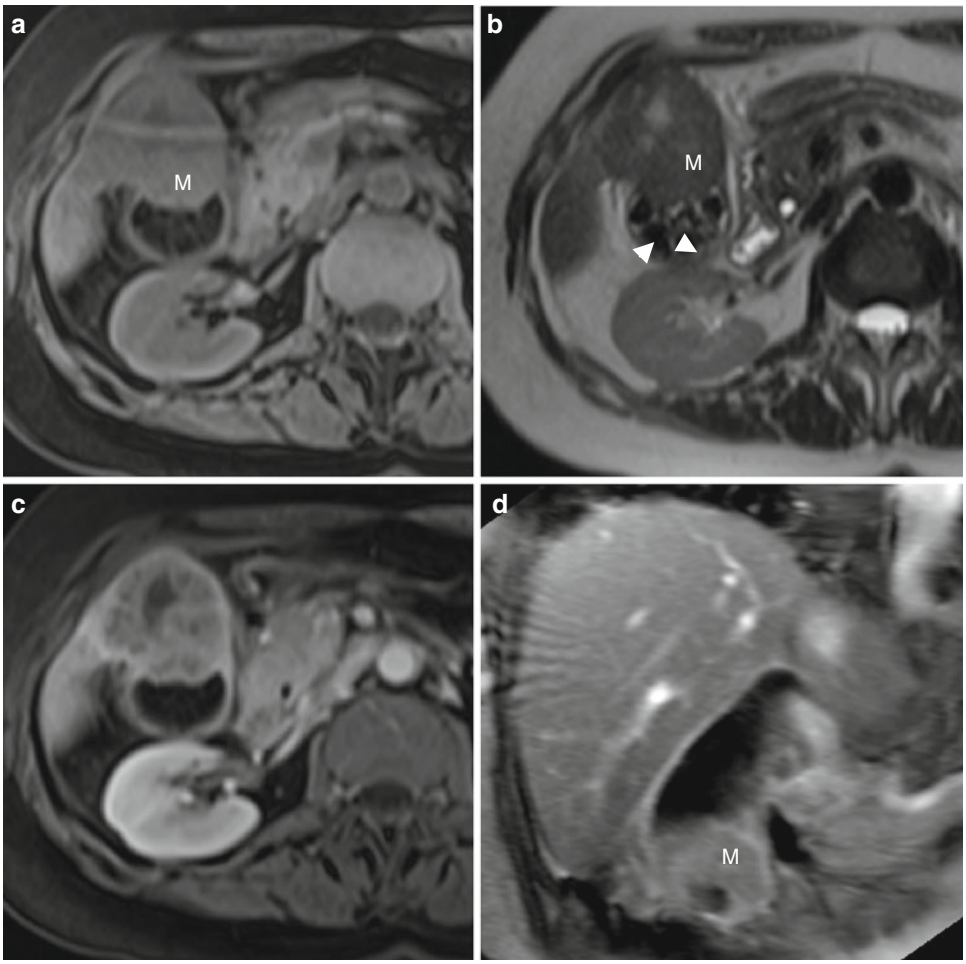

Fig. 11 A 73-year-old female with primary gallbladder carcinoma. **a** T1 weighted demonstrates an isointense mass-like (M) thickening of the gallbladder fundus with a central hypointense area probably related to central necrosis. **b** The mass is hypointense in T2-weighted images with a central hyperintense area. There are innumerable gallstones (*arrowheads*). **c** There is enhancement of the mass after contrast administration enhancement administration consistent with gallbladder carcinoma. **d** Oblique coronal image depicts the mass-like thickening of the gallbladder fundus

gallbladder cancer is difficult. T1-weighted images showed low signal intensity on fat-suppression images and high signal intensity on T2-weighted fat-suppression sequence. T2-weighted images show homogenous signal slightly hypointense compared to gallbladder carcinoma with presence of enlarged lymph nodes.

7 Conclusion and Future Directions

The role of MRCP for the diagnosis of biliary malignancies will further expand due to technological advances both in acquisition and in post-processing software. Functional MRCP using hepatobiliary contrast agents and MRI-based assessment of tumor angiogenesis will further progress. Image resolution and SNR will increase with the development of dedicated MR coils. These current developments will provide a unique opportunity for excellent depiction of anatomic and pathophysioplogical information using MRI.

References

1. Domagk D et al (2004) Endoscopic retrograde cholangiopancreatography, intraductal ultrasonography, and magnetic resonance cholangiopancreatography in bile duct strictures: a prospective comparison of imaging diagnostics with histopathological correlation. Am J Gastroenterol 99:1684–1689
2. Fernandez-Esparrach G et al (2007) Comparison of endoscopic ultrasonography and magnetic resonance cholangiopancreatography in the diagnosis of pancreatobiliary diseases: a prospective study. Am J Gastroenterol 102:1632–1639
3. Hekimoglu K et al (2008) MRCP vs. ERCP in the evaluation of biliary pathologies: review of current literature. J Dig Dis 9:162–169
4. Hintze RE et al (1997) Clinical significance of magnetic resonance cholangiopancreatography (MRCP) compared to endoscopic retrograde cholangiopancreatography (ERCP). Endoscopy 29:182–187
5. Kaltenthaler EC et al (2006) MRCP compared to diagnostic ERCP for diagnosis when biliary obstruction is suspected: a systematic review. BMC Med Imaging 6:9
6. Park MS et al (2004) Differentiation of extrahepatic bile duct cholangiocarcinoma from benign stricture: findings at MRCP versus ERCP. Radiology 233:234–240

7. Schulte B, Beyer D, Wedekind G, Meuser W (1998) Single shot MRI cholangiopancreatography (MRCP) with a "fast acquisition spin echo" sequence (FASE). Replacement of ERCP? Aktuelle Radiol 8:18–24
8. Lee NK et al (2009) Biliary MR imaging with Gd-EOB-DTPA and its clinical applications. Radiographics 29:1707–1724
9. Park MS, Yu JS, Lee JH, Kim KW (2007) Value of manganese-enhanced T1-and T2-weighted MR cholangiography for differentiating cystic parenchymal lesions from cystic abnormalities which communicate with bile ducts. Yonsei Med J 48:1072–1074
10. Holzapfel K, Breitwieser C, Prinz C, Rummeny EJ, Gaa J (2007) Contrast-enhanced magnetic resonance cholangiography using gadolinium-EOB-DTPA. Preliminary experience and clinical applications. Radiologe 47:536–544
11. Fayad LM, Kamel IR, Mitchell DG, Bluemke DA (2005) Functional MR cholangiography: diagnosis of functional abnormalities of the gallbladder and biliary tree. AJR Am J Roentgenol 184:1563–1571
12. Aduna M et al (2005) Bile duct leaks after laparoscopic cholecystectomy: value of contrast-enhanced MRCP. Abdom Imaging 30:480–487
13. Khan SA, Thomas HC, Davidson BR, Taylor-Robinson SD (2005) Cholangiocarcinoma. Lancet 366:1303–1314
14. Soyer P, Lacheheb D, Levesque M (1993) False-positive CT portography: correlation with pathologic findings. AJR Am J Roentgenol 160:285–289
15. Shaib YH, El-Serag HB, Davila JA, Morgan R, McGlynn KA (2005) Risk factors of intrahepatic cholangiocarcinoma in the United States: a case-control study. Gastroenterology 128:620–626
16. Welzel TM et al (2007) Risk factors for intrahepatic and extrahepatic cholangiocarcinoma in the United States: a population-based case-control study. Clin Gastroenterol Hepatol 5:1221–1228
17. Paulson EK et al (1992) CT arterial portography: causes of technical failure and variable liver enhancement. AJR Am J Roentgenol 159:745–749
18. Kuhn M, Neufang KF, Gross-Fengels W, Zieren U (1992) Liver angiography–technique, indications and significance in focal liver processes. Aktuelle Radiol 2:285–292
19. Yamasaki S (2003) Intrahepatic cholangiocarcinoma: macroscopic type and stage classification. J Hepatobiliary Pancreat Surg 10:288–291
20. Menias CO et al (2008) Mimics of cholangiocarcinoma: spectrum of disease. Radiographics 28:1115–1129
21. Peporte AR, Sommer WH, Nikolaou K, Reiser MF, Zech CJ (2012) Imaging features of intrahepatic cholangiocarcinoma in Gd-EOB-DTPA-enhanced MRI. *Eur J Radiol*
22. Maetani Y et al (2001) MR imaging of intrahepatic cholangiocarcinoma with pathologic correlation. AJR Am J Roentgenol 176:1499–1507
23. Han JK, Lee JM (2004) Intrahepatic intraductal cholangiocarcinoma. Abdom Imaging 29:558–564
24. Kim JE et al (2010) Differentiation of intraductal growing-type cholangiocarcinomas from nodular-type cholangiocarcinomas at biliary MR imaging with MR cholangiography. Radiology 257:364–372
25. Bismuth H, Nakache R, Diamond T (1992) Management strategies in resection for hilar cholangiocarcinoma. Ann Surg 215:31–38
26. Vanderveen KA, Hussain HK (2004) Magnetic resonance imaging of cholangiocarcinoma. Cancer Imaging 4:104–115
27. Cui XY, Chen HW (2010) Role of diffusion-weighted magnetic resonance imaging in the diagnosis of extrahepatic cholangiocarcinoma. World J Gastroenterol 16:3196–3201
28. Manfredi R et al (2003) MR imaging and MRCP of hilar cholangiocarcinoma. Abdom Imaging 28:319–325
29. Guthrie JA, Ward J, Robinson PJ (1996) Hilar cholangiocarcinomas: T2-weighted spin-echo and gadolinium-enhanced FLASH MR imaging. Radiology 201:347–351
30. Kassahun WT, Hauss J (2008) Management of combined hepatocellular and cholangiocarcinoma. Int J Clin Pract 62:1271–1278
31. de Campos RO et al (2012) Combined hepatocellular carcinoma-cholangiocarcinoma: report of MR appearance in eleven patients. J Magn Reson Imaging 36:1139–1147
32. Hwang J et al (2012) Differentiating combined hepatocellular and cholangiocarcinoma from mass-forming intrahepatic cholangiocarcinoma using gadoxetic acid-enhanced MRI. J Magn Reson Imaging 36:881–889
33. Park HJ, Kim YK, Park MJ, Lee WJ (2012) Small intrahepatic mass-forming cholangiocarcinoma: target sign on diffusion-weighted imaging for differentiation from hepatocellular carcinoma. Abdom Imaging
34. Riopel MA, Klimstra DS, Godellas CV, Blumgart LH, Westra WH (1997) Intrabiliary growth of metastatic colonic adenocarcinoma: a pattern of intrahepatic spread easily confused with primary neoplasia of the biliary tract. Am J Surg Pathol 21:1030–1036
35. Medina V et al (2003) Primary biliary tract malignant melanoma: US, CT, and MR findings. Abdom Imaging 28:842–846
36. Vitellas KM et al (2000) Radiologic manifestations of sclerosing cholangitis with emphasis on MR cholangiopancreatography. Radiographics 20:959–975; quiz 1108–1109, 1112
37. Park MS et al (2001) Recurrent pyogenic cholangitis: comparison between MR cholangiography and direct cholangiography. Radiology 220:677–682
38. Lai EC, Lau WY (2006) Mirizzi syndrome: history, present and future development. ANZ J Surg 76:251–257
39. Choi BW et al (2000) Radiologic findings of Mirizzi syndrome with emphasis on MRI. Yonsei Med J 41:144–146
40. Finkelberg DL, Sahani D, Deshpande V, Brugge WR (2006) Autoimmune pancreatitis. N Engl J Med 355:2670–2676
41. Kim JH et al (2002) Differential diagnosis of periampullary carcinomas at MR imaging. Radiographics 22:1335–1352
42. Kim JY et al (2007) Contrast-enhanced MRI combined with MR cholangiopancreatography for the evaluation of patients with biliary strictures: differentiation of malignant from benign bile duct strictures. J Magn Reson Imaging 26:304–312
43. Soto JA et al (2000) Biliary obstruction: findings at MR cholangiography and cross-sectional MR imaging. Radiographics 20:353–366
44. Wu DS, Chen WX, Wang XD, Acharya R, Jiang XH (2012) Pancreaticobiliary duct changes of periampullary carcinomas: quantitative analysis at MR imaging. Eur J Radiol 81:2112–2117
45. Chung YE et al (2011) Differentiation of benign and malignant ampullary obstructions on MR imaging. Eur J Radiol 80:198–203
46. Chung YE et al (2010) Differential features of pancreatobiliary- and intestinal-type ampullary carcinomas at MR imaging. Radiology 257:384–393
47. Irie H et al (2002) MR imaging of ampullary carcinomas. J Comput Assist Tomogr 26:711–717
48. Jang KM et al (2012) Added value of diffusion-weighted MR imaging in the diagnosis of ampullary carcinoma. Radiology
49. Roberts JW, Daugherty SF (1986) Primary carcinoma of the gallbladder. Surg Clin North Am 66:743–749
50. Tazuma S, Kajiyama G (2001) Carcinogenesis of malignant lesions of the gall bladder. The impact of chronic inflammation and gallstones. Langenbecks Arch Surg 386:224–229

51. Sheth S, Bedford A, Chopra S (2000) Primary gallbladder cancer: recognition of risk factors and the role of prophylactic cholecystectomy. Am J Gastroenterol 95:1402–1410
52. Weiss KM, Ferrell RE, Hanis CL, Styne PN (1984) Genetics and epidemiology of gallbladder disease in New World native peoples. Am J Hum Genet 36:1259–1278
53. Sameshima Y, Uchimura M, Muto Y, Maeda J, Tsuchiyama H (1987) Coexistent carcinoma in congenital dilatation of the bile duct and anomalous arrangement of the pancreatico-bile duct. Carcinogenesis of coexistent gall bladder carcinoma. Cancer 60:1883–1890
54. Reid KM, Ramos-De la Medina A, Donohue JH (2007) Diagnosis and surgical management of gallbladder cancer: a review. J Gastrointest Surg 11:671–681
55. Bartlett DL (2000) Gallbladder cancer. Semin Surg Oncol 19:145–155
56. Levy AD, Murakata LA, Rohrmann CA Jr (2001) Gallbladder carcinoma: radiologic-pathologic correlation. Radiographics 21:295–314; questionnaire, 549–555
57. Gore RM, Yaghmai V, Newmark GM, Berlin JW, Miller FH (2002) Imaging benign and malignant disease of the gallbladder. Radiol Clin North Am 40(6):1307–23
58. van Breda Vriesman AC, Engelbrecht MR, Smithuis RH, Puylaert JB (2007) Diffuse gallbladder wall thickening: differential diagnosis. AJR Am J Roentgenol 188, 495–501
59. Catalano OA et al (2008) MR imaging of the gallbladder: a pictorial essay. Radiographics 28, 135–155; quiz 324
60. Yoshimitsu K et al (1997) Dynamic MRI of the gallbladder lesions: differentiation of benign from malignant. J Magn Reson Imaging 7:696–701
61. Mani H et al (2010) Gall bladder and extrahepatic bile duct lymphomas: clinicopathological observations and biological implications. Am J Surg Pathol 34:1277–1286
62. Ono A et al (2009) Primary malignant lymphoma of the gallbladder: a case report and literature review. Br J Radiol 82:e15–e19